

César Augusto Barrero Meneses
Edson Passamani Caetano · Claudia E. Rodríguez Torres
Carmen Pizarro · Ligia Edith Zamora Alfonso *Editors*

LACAME 2012

Proceedings of the 13th Latin American
Conference on the Applications of the
Mössbauer Effect, (LACAME 2012)
held in Medellín, Colombia,
November 11–16, 2012

LACAME 2012

C.A. Barrero Meneses • E. Passamani Caetano
C.E. Rodríguez Torres • C. Pizarro
L.E. Zamora Alfonso
Editors

LACAME 2012

Proceedings of the 13th Latin American
Conference on the Applications of the
Mössbauer Effect, (LACAME 2012)
held in Medellín, Colombia,
November 11–16, 2012

Previously published in *Hyperfine Interactions*
Volume 224, 2014

 Springer

Editors

César Augusto Barrero Meneses
Instituto de Física
Universidad de Antioquia
Medellín, Colombia

Edson Passamani Caetano
Centro de Ciências Exatas
Departamento de Física
Universidade Federal do Espírito Santo
Vitória ES, Brazil

Claudia Elena Rodríguez Torres
Departamento de Física y Ciencias Exactas
Universidad Nacional de La Plata
La Plata, Argentina

Carmen Pizarro
Facultad de Química y Biología
Universidad de Santiago de Chile
Santiago, Chile

Ligia Edith Zamora Alfonso
Departamento de Física
Universidad del Valle
Cali, Colombia

ISBN 978-94-007-6481-1 ISBN 978-94-007-6482-8 (eBook)
DOI 10.1007/978-94-007-6482-8
Springer Dordrecht Heidelberg New York London

Library of Congress Control Number: 2014935866

© Springer Science+Business Media Dordrecht 2014

This work is subject to copyright. All rights are reserved by the Publisher, whether the whole or part of the material is concerned, specifically the rights of translation, reprinting, reuse of illustrations, recitation, broadcasting, reproduction on microfilms or in any other physical way, and transmission or information storage and retrieval, electronic adaptation, computer software, or by similar or dissimilar methodology now known or hereafter developed. Exempted from this legal reservation are brief excerpts in connection with reviews or scholarly analysis or material supplied specifically for the purpose of being entered and executed on a computer system, for exclusive use by the purchaser of the work. Duplication of this publication or parts thereof is permitted only under the provisions of the Copyright Law of the Publisher's location, in its current version, and permission for use must always be obtained from Springer. Permissions for use may be obtained through RightsLink at the Copyright Clearance Center. Violations are liable to prosecution under the respective Copyright Law.

The use of general descriptive names, registered names, trademarks, service marks, etc. in this publication does not imply, even in the absence of a specific statement, that such names are exempt from the relevant protective laws and regulations and therefore free for general use.

While the advice and information in this book are believed to be true and accurate at the date of publication, neither the authors nor the editors nor the publisher can accept any legal responsibility for any errors or omissions that may be made. The publisher makes no warranty, express or implied, with respect to the material contained herein.

Printed on acid-free paper

Springer is part of Springer Science+Business Media (www.springer.com)

Preface

Published online: 28 March 2013

© Springer Science+Business Media Dordrecht 2013

Mössbauer Spectroscopy is an experimental technique based on the nuclear resonant emission and absorption of gamma rays. It was discovered in 1958 by Professor Rudolf Mössbauer who received the Nobel Prize for Physics in 1961. Due to its high sensitivity to the local physical properties of the systems under study, the technique has proven to be very useful in several areas of scientific and technological research.

The “Latin American Conference on the Applications of the Mössbauer Effect-LACAME” is a series of conferences started in 1988 in Rio de Janeiro and has grown steadily since then, changing every 2 years the venue from different nations in which Mössbauer research laboratories exist. The purposes of LACAME are to bring together the Latin American and the International community, to promote activities of basic and applied research, to encourage participation and interaction among students, young and senior researchers, and to strengthen international cooperation around the field. LACAME is the best opportunity to share experiences gained in the process by each of the different countries as well as a good opportunity for the students of Latin American countries to discuss their researches with specialists of Latin America and abroad that work with the same experimental characterization technique. Topics addressed in these conferences include Advances in Experimentation and Data Processing, Amorphous, Nanocrystals and Nanoparticles, Applications in Soils, Mineralogy, Geology and Archaeology, Biological and Medical Applications, Catalysis, Corrosion and Environment, Chemical Applications, Structure and Bonding, Industrial Applications, Magnetism and Magnetic Materials, Multilayers, Thin Films and Artificially Structured Materials, Physical Metallurgy and Materials Science, and others related with the use of Mössbauer spectroscopy.

In 2012, the Institute of Physics at the Universidad de Antioquia (Medellín-Colombia) had the privilege to lead the planning and development of this important academic event in cooperation with Planetario de Medellín “Jesús Emilio Ramírez González” and Parque Explora. In order to ensure the continuity of the Latin American Mössbauer Community, in LACAME-2012 different activities were programmed encouraging the creation of the new generation for Mössbauer spectroscopy in Latin America. Therefore, the “International School on Recent Advances in Mössbauer Spectroscopy”, the “Rudolf Mössbauer Latin American Thesis Award”, and the “Best Presentation Award” were specially organized to promote active participation of young scientists. Additionally, internationally recognized experts of the highest scientific level as well as young prominent researchers from Latin America were invited as Speakers and also as Tutors of the International School.

The Organizing Committee decided to honor the outstanding scientific contributions of Prof. R. Mössbauer, who passed away in 2011, through the “Rudolf Mössbauer Latin American Thesis Award-2012”. Also, several academic sessions were devoted to honor the memory of our friends and colleagues Profs. Fernando González-Jiménez (Venezuela), I. P. Suzdalev (Russia), A. Vértes (Hungary) and H. Rechenberg (Brazil), who regrettably passed away in the last years. Soon after finishing the Conference, we received the sad news, that our colleague and friend Dra. Judith Dessimoni (Argentina) died on November 26 of 2012. We certainly shall miss all of them.

Medellín, known as the ‘city of the eternal spring’, welcomed the Mössbauer community. Nowadays, this city has been chosen as the most innovative city in the world by the Urban Land Institute, Citigroup and The Wall Street Journal. It is becoming the destination of choice for many new and seasoned visitors. It is a vibrant, vital and rapidly developing place that offers an excellent platform for varied activity as tourism, conventions and academic conferences.

We are convinced that the readers will enjoy the scientific contributions published in the present volume, which give an overview of the science currently done around the Applications of the Mössbauer Effect. We would like to express our deep gratitude to all the institutions supporting LACAME 2012, and thank all the presenters, participants, and members of the Organizing, Latin American and Scientific Committees for making this conference possible. The conference counted with the presence of 131 participants, mostly students, including leading researchers in the field coming from 16 countries of Latin America, Europe, Asia, and North America. Over 120 works were presented both domestic and from abroad; all of them with excellent scientific quality and valuable contributions to the field. In this proceeding volume, the papers accepted for publication in the *Journal of Hyperfine Interactions* were submitted through the online system via editorial management newly provided by Springer.

C.A. Barrero Meneses and J. Mazo-Zuluaga (Chairs)



XIII Latin American Conference on the Applications of the Mössbauer Effect LACAME-2012
Universidad de Antioquia - Planetario de Medellín - Colombia
11-16 November 2012



Contents

Chairmen and committees	xiii
Mössbauer investigation of the reaction of ferrate(VI) with sulfamethoxazole and aniline in alkaline medium	1
V.K. Sharma, Z. Homonnay, K. Siskova, L. Machala, and R. Zboril	
Analysis of broadened Mössbauer spectra using simple mathematical functions	9
A. Cabral-Prieto	
Mössbauer and vibrational DOS studies of diluted magnetic tin oxides and nano iron oxides	19
K. Nomura, A.I. Rykov, A.M. Mudarra Navarro, C.E. Rodriguez Torres, L.A. Errico, C.A. Barrero, and Y. Yoda	
Effect of sintering conditions on the magnetic and structural properties of $Fe_{0.6}Mn_{0.1}Al_{0.3}$ synthesized by mechanical alloying	29
J.M. Marín, Y.A. Rojas, G.A. Pérez Alcázar, B. Cruz, and M.H. Medina Barreto	
Design of an Auger Electron Mössbauer Spectrometer (AEMS) using a modified cylindrical mirror analyzer	37
F. Moutinho, C. Rojas, and L. D'Onofrio	
^{57}Fe Mössbauer spectroscopy studies of Tektites from Khon Kaen, Ne Thailand	45
B.F.O. Costa, G. Klingelhöfer, and E.I. Alves	
Formation of magnetic nanoparticles studied during the initial synthesis stage	51
M. Kraken, I.-C. Masthoff, A. Borchers, F.J. Litterst, and G. Garnweitner	
Implementation of a preamplifier-amplifier system for radiation detectors used in Mössbauer spectroscopy	59
A.A. Velásquez and M. Arroyave	
Self-tuning digital Mössbauer detection system	67
A. Veiga, C.M. Grunfeld, G.A. Pasquevich, P. Mendoza Zélis, N. Martínez, and F.H. Sánchez	

Formation of nanostructured ω-Al₇Cu₂Fe crystalline phase by the ball milling technique	77
M.Z. Pinto, M. Pillaca, C.V. Landauro, J. Quispe-Marcatoma, C. Rojas-Ayala, V.A. Peña Rodríguez, and E. Baggio-Saitovitch	
Mössbauer study of intermediate superparamagnetic relaxation of maghemite (γ-Fe₂O₃) nanoparticles	83
J.A. Ramos Guivar, A. Bustamante, J. Flores, M. Mejía Santillan, A.M. Osorio, A.I. Martínez, L. De Los Santos Valladares, and C.H.W. Barnes	
Mössbauer study of a Fe₃O₄/PMMA nanocomposite synthesized by sonochemistry	93
H. Martínez, L. D’Onofrio, and G. González	
Characterization of iron in airborne particulate matter	103
F.V.F. Tavares, J.D. Ardisson, P.C.H. Rodrigues, W. Brito, W.A.A. Macedo, and V.M.F. Jacomino	
Oxidation states of iron as an indicator of the techniques used to burn clays and handcraft archaeological Tupiguarani ceramics by ancient human groups in Minas Gerais, Brazil	115
D.L. Floresta, J.D. Ardisson, M. Fagundes, J.D. Fabris, and W.A.A. Macedo	
Comparison of methods to obtain ash from coal of the Southwest of Colombia	125
G. Medina, J.A. Tabares, G.A. Pérez Alcazar, and J.M. Barraza	
Whiteness process of tile ceramics: using a synthetic flow as a modifier agent of color firing	131
G.R. dos Santos, M.C. Pereira, M. Olzon-Dionysio, S.D. de Souza, and M.R. Morelli	
Minerals of a soil developed in the meteoritic crater of Carancas, Peru, and evidences of phase changes on the impact event	137
M.L. Cerón Loayza and J.A. Bravo Cabrejos	
Iron-bearing minerals in ashes emanated from Osorno volcano, in Chile	147
A.C. Silva, M. Escudey, J.E. Förster, C. Pizarro, J.D. Ardisson, U.M. Barral, M.C. Pereira, and J.D. Fabris	
A pre-Columbian copper alloy smelting furnace: Mössbauer and XRD study of the firing conditions	155
F.M. Hayashida, D. Killick, I. Shimada, W. Häusler, F.E. Wagner, and U. Wagner	
Structural, calorimetric and magnetic properties study of the Cu_{0,91}Fe_{0,09}O system	165
H.D. Colorado, J.S.T. Hernandez, G.A.P. Alcázar, and A. Bolaños	
Synthesis and characterization of uncoated and gold-coated magnetite nanoparticles	173
L. León-Félix, J. Chaker, M. Parise, J.A.H. Coaquira, L. De Los Santos Valladares, A. Bustamante, V.K. Garg, A.C. Oliveira, and P.C. Morais	

Size dependence of the magnetic and hyperfine properties of nanostructured hematite (α-Fe₂O₃) powders prepared by the ball milling technique	183
J. André-Filho, L. León-Félix, J.A.H. Coaquira, V.K. Garg, and A.C. Oliveira	
Magnetic composites from minerals: study of the iron phases in clay and diatomite using Mössbauer spectroscopy, magnetic measurements and XRD.....	191
M. Cabrera, J.C. Maciel, J. Quispe-Marcátoma, B. Pandey, D.F.M. Neri, F. Soria, E. Baggio-Saitovitch, and L.B. de Carvalho Jr	
Enhancing vibration measurements by Mössbauer effect.....	199
G.A. Pasquevich, A. Veiga, P. Mendoza Zélis, N. Martínez, M. Fernández van Raap, and F.H. Sánchez	
Preparation and characterization of cobalt ferrite nanoparticles coated with fucan and oleic acid.....	211
P.L. Andrade, V.A.J. Silva, J.C. Maciel, M.M. Santillan, N.O. Moreno, L. De Los Santos Valladares, A. Bustamante, S.M.B. Pereira, M.P.C. Silva, and J. Albino Aguiar	
Magnetic and Mössbauer studies of fucan-coated magnetite nanoparticles for application on antitumoral activity.....	221
V.A.J. Silva, P.L. Andrade, A. Bustamante, L. de los Santos Valladares, M. Mejia, I.A. Souza, K.P.S. Cavalcanti, M.P.C. Silva, and J. Albino Aguiar	
Structural and hyperfine properties of Mn and Co-incorporated akaganeites	233
A.E. Tufo, K.E. García, C.A. Barrero, and E.E. Sileo	
Fe²⁺-Mg order–disorder study in orthopyroxenes from São João Nepomuceno (IVA) iron meteorite.....	245
E. dos Santos, R.B. Scorzelli, M.E. Varela, and P. Munayco	
⁵⁷Fe Mössbauer spectroscopy studies of chondritic meteorites from the Atacama Desert, Chile: Implications for weathering processes	251
P. Munayco, J. Munayco, M. Valenzuela, P. Rochette, J. Gattacceca, and R.B. Scorzelli	
Mössbauer study of the inorganic sulfur removal from coals.....	257
F. Reyes Caballero and S.A. Martínez Ovalle	
Mössbauer analysis of coal coke samples from Samacá, Boyacá, Colombia ...	265
W.A. Pacheco Serrano, D. Quintão Lima, and J.D. Fabris	
Erratum to: Mössbauer analysis of coal coke samples from Samacá, Boyacá, Colombia	271
W.A. Pacheco Serrano, D. Quintão Lima, and J.D. Fabris	
Indoor atmospheric corrosion of conventional weathering steels in the tropical atmosphere of Panama	273
J.A. Jaén, J. Iglesias, and O. Adames	

Structural and magnetic characterization of the “GASPAR” meteorite from Betétiva, Boyacá, Colombia	283
L.M. Flor Torres and G.A. Pérez Alcazar	
Iron nano-clusters in ytterbium films: a ⁵⁷Fe Mössbauer spectroscopic study	293
C. Rojas-Ayala, W.T. Herrera, I.S. Dinóla, M. Kraken, E.C. Passamani, E. Baggio-Saitovitch, and F.J. Litterst	
Processing of gadolinium–iron garnet under non-equilibrium conditions	301
S.C. Zanatta, F.F. Ivashita, K.L. da Silva, C.F.C. Machado, and A. Paesano Jr.	
Effect of boron in Fe₇₀Al₃₀ nanostructured alloys produced by mechanical alloying	307
M.M. Rico, G.A. Pérez Alcázar, and J.M. Greneche	
Mössbauer and X-ray study of the Fe₆₅Ni₃₅ invar alloy obtained by mechanical alloying	317
R.R. Rodriguez, J.L. Valenzuela, J.A. Tabares, and G.A. Pérez Alcázar	

Chairmen and committees

Published online: 28 March 2013
© Springer Science+Business Media Dordrecht 2013

Committees

Chairpersons

C.A. Barrero Meneses (UdeA)
J. Mazo-Zuluaga (UdeA)

Local Organizing Committee

K.E. García Téllez (UdeA)
J.A. Osorio (UdeA)
A.L. Morales Aramburo (UdeA)
J. Restrepo Cárdenas (UdeA)
O.L. Arnache Olmos (UdeA)
J.E. Tobón (UdeA)
A.A. Velásquez Torres (EAFIT)
F.R. Pérez (UPB)
G.A. Pérez Alcázar (UV)
L.E. Zamora Alfonso (UV)
Y.A. Rojas Martínez (UT)
D. Oyola Lozano (UT)
H. Bustos Rodríguez (UT)
B.C. Londoño (UTP)
R. Rodríguez (UAO)

Latin American Committee

E.M. Baggio Saitovitch (CBPF-Brazil)
F. González Jiménez (UCV-Venezuela)
G.A. Pérez Alcázar (UV-Colombia)
J.A. Jaén (UP-Panamá)

N.R. Furet Bridón (CNIC-Cuba)
N. Nava (IMP-México)
R.C. Mercader (UNLP-Argentina)
V.A. Peña Rodríguez (UNMSM-Perú)
C. Pizarro (USACH-Chile)

Scientific Committee

E.M. Baggio Saitovitch (CBPF-Brazil)
R.C. Mercader (UNLP-Argentina)
F.H. Sánchez (UNLP-Argentina)
C. Saragovi (CNEA-Argentina)
C. Partiti (USP-Brazil)
C. Larica (UFES-Brazil)
E.C. Passamani (UFES-Brazil)
C.A. Barrero Meneses (UdeA-Colombia)
N.R. Furet Bridón (CNIC-Cuba)
J.A. Jaén (UP-Panamá)
A. Bustamante Domínguez (UNMSM-Perú)
J.R. Gancedo (IQFR-Spain)

SPONSORS

Universidad de Antioquia
Planetario de Medellín “Jesús Emilio Ramírez González”
Parque Explora
COLCIENCIAS
IOP Publishing
Universidad del Tolima
Universidad EAFIT
Universidad Tecnológica de Pereira
Medellín Convention and Visitors Bureau
Alcaldía de Medellín
Centro Latinoamericano de Física-CLAF
WissEL GmbH
Embajada de Francia en Colombia
Sociedad Colombiana de Física
Universidad Pontificia Bolivariana
Universidad Autónoma de Occidente-Cali
SENA
Springer Science, Business Media–The Netherlands

Mössbauer investigation of the reaction of ferrate(VI) with sulfamethoxazole and aniline in alkaline medium

Virender K. Sharma · Zoltan Homonnay ·
Karolina Siskova · Libor Machala · Radek Zboril

Published online: 13 February 2013

© Springer Science+Business Media Dordrecht 2013

Abstract Mechanisms on the oxidation of sulfamethoxazole (SMX) and aniline by ferrate(VI) ($\text{Fe}^{\text{VI}}\text{O}_4^{2-}$, Fe(VI)) in alkaline medium suggested the formation of Fe(VI)-SMX or Fe(VI)-aniline intermediates, respectively. Fe(V) and Fe(IV) as other intermediate iron species have also been proposed in the mechanism. In this paper, rapid freeze Mössbauer spectroscopy was applied in rapidly frozen samples to explore intermediate iron species in the reactions of SMX and aniline with Fe(VI) . In both reactions, Fe(VI)-SMX and Fe(VI)-aniline intermediates were not seen in second-minute time scale. Fe(V) and Fe(IV) were also not observed. Fe(III) was the only final species of the reactions.

Keywords Ferrate · High-valent iron species · Fe(II) · Fe(III) · Antibiotics · Electron-transfer · Rapid-freeze technique · Mössbauer spectroscopy

Thirteenth Latin American Conference on the Applications of the Mössbauer Effect, LACAME 2012, Medellín, Columbia, 11–16 November 2012.

V. K. Sharma (✉)

Center of Ferrate Excellence and Chemistry Department,
Florida Institute of Technology, 150 West University Boulevard,
Melbourne, FL 32901, USA
e-mail: vsharma@fit.edu

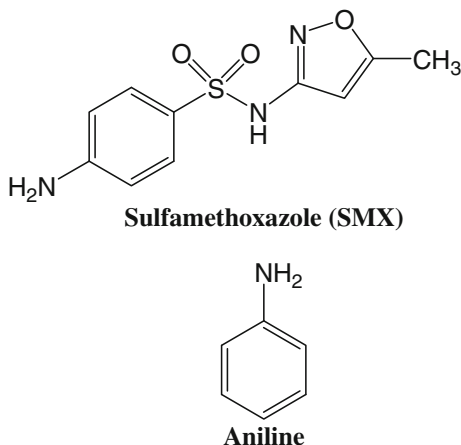
Z. Homonnay

Laboratory of Nuclear Chemistry, Institute of Chemistry,
Eotvos Lorand University, Pazmany P.s. 1/A, Budapest, Hungary

K. Siskova · L. Machala · R. Zboril

Regional Center of Advanced Materials and Technologies,
Palacky University in Olomouc, 17. listopadu 1192/12,
771 46 Olomouc, Czech Republic

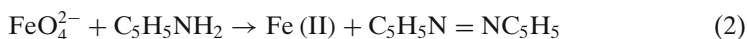
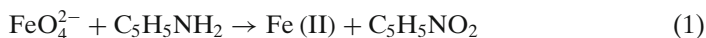
Fig. 1 Structures of sulfamethoxazole (SMX) and aniline



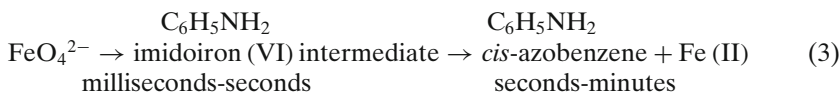
1 Introduction

The application of potassium ferrate(VI) (K_2FeO_4 , Fe(VI)) in water and wastewater treatment is attracting increasing interest [1–8]. Fe(VI) is a strong oxidizing agent with a standard reduction potential of 2.20 V under acidic conditions, however it is relatively mild oxidant in the basic conditions with a standard reduction potential of 0.72 V [9]. Like ozone, Fe(VI) does not produce carcinogenic bromate ion in treatment of Br^- containing water [7]. Because of growing concern of chlorine disinfection by-products (DBPs), Fe(VI) shows promise as an alternative disinfectant [10]. Fe(VI) can also be an effective oxidant for removal of organic micropollutants such as estrogens and certain pharmaceuticals [11–17]. No antibacterial activity against *E. coli* after complete removal of antibiotic, trimethoprim by Fe(VI) was observed [14].

The understanding of the mechanisms of oxidation reactions carried out by Fe(VI) is in progress [18, 19]. In our laboratory, we are attempting to advance knowledge on the mechanism of oxidation of antibiotics by Fe(VI) [14, 20]. The present paper deals with antibiotic, sulfamethoxazole (SMX), which consists of two moieties, an aniline ring and a five-membered heterocyclic aromatic group, connected to both sides of the sulfonamide linkage ($-NH-SO_2-$) (Fig. 1). In the proposed mechanism of Fe(VI) with SMX, intermediate iron in +4 oxidation state has been suggested [20]. However, no direct evidence was provided to confirm this intermediate iron species. Furthermore, a recent study proposed Fe(VI)-SMX intermediate species and analyzed their kinetics results based on this assumption [15]. Moreover, studies on aniline, a substructure molecule of SMX (see Fig. 1) have also been performed [21–23]. Under condition of using excess molar amounts of Fe(VI) to aniline, nitrobenzene was the product of the reaction (1) while azobenzene was formed when excess aniline was used (2).



A free radical mechanism for the reaction, based on EPR measurements was proposed when excess amounts of aniline to Fe(VI) was used [21]. In this free radical mechanism, FeO_4^{3-} (Fe(V)) was also the intermediate high-valent iron species. However, a study under similar experimental conditions contradicted the free radical based mechanism, and the imidoiron(VI) intermediate as the intermediate was suggested before the formation of final product, *cis*-azobenzene (3) [21].



In the last few years, we are attempting to explore mechanism of the oxidation reactions of Fe(VI) using the Mössbauer spectroscopy in order to establish any intermediate iron(VI)-substrate species or to distinguish one-electron steps ($\text{Fe(VI)} \rightarrow \text{Fe(IV)} \rightarrow \text{Fe(III)}$) and two-electron steps ($\text{Fe(VI)} \rightarrow \text{Fe(IV)} \rightarrow \text{Fe(II)}$) [5, 24, 25]. The oxidation states of iron can be determined unequivocally by the Mössbauer technique [26] and therefore, any intermediate iron species of the reaction may be known. In the current paper, we have applied Mössbauer technique to the reactions of Fe(VI) with SMX and aniline to learn about the mechanism of the reactions.

2 Experimental methods

The samples for Mössbauer spectroscopy were prepared by mixing solutions of 0.2 M Fe(VI) with either SMX or aniline in 10 M NaOH and in 0.01 M phosphate buffer (pH 11.0). The experiments at pH 9.0 for the reaction of Fe(VI) with aniline were performed under anaerobic solutions in which 0.2 M Fe(VI) (a ferrate(VI) sample enriched in ^{57}Fe isotope) and 0.2 M aniline were mixed to achieve the molar ratio 1:1. Anaerobic conditions were obtained by degassing with a stream of nitrogen to remove oxygen prior to mixing them together and the volume used for each solution was 100 μL . The mixing of solutions was performed in a Mössbauer sample holder (i.e., in a tiny bowl) within second time scale. The sample holder was then immersed into liquid nitrogen (78 K). The cooling rate provided by this method preserves the original structure of the solution and iron species in the liquid state [25].

The transmission ^{57}Fe Mössbauer spectra were recorded at $T = 100$ K using a Mössbauer spectrometer in a constant acceleration mode with a $^{57}\text{Co(Rh)}$ source and velocity range from -5 to 5 mm/s. The isomer shift values are given relative to metallic alpha iron at room temperature. The Mössbauer spectra were evaluated assuming Lorentzian line shapes using the least squares method with the help of the MossWinn^R code. It was expected that the effects of non-ideal absorber thickness and variable recoil-free fractions for iron atoms in non-equivalent structural sites are all within experimental error.

3 Results and discussion

Initially, solid SMX was added into 0.1 M Fe(VI) solution in 10 M NaOH solution. It was expected that such high concentration of hydroxide would stabilize any intermediate Fe(V)/Fe(IV) species [27]. As shown in Fig. 2, the Mössbauer

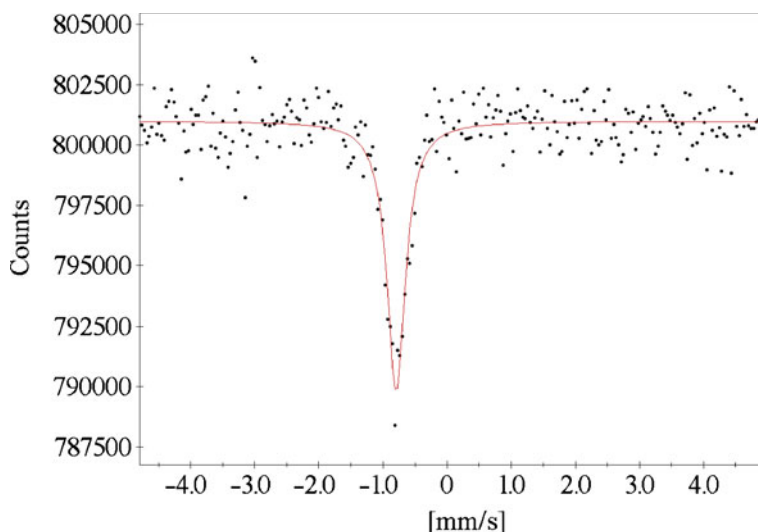


Fig. 2 Mössbauer spectrum of the frozen solution of the mixture of 0.1 M Fe(VI) and solid SMX

spectrum of the frozen solution showed a single component having isomer shift of -0.82 mm/s and this represents non reacted Fe(VI). The Fe(V) and Fe(IV) species as intermediates of the reaction between Fe(VI) and SMX were not seen. Furthermore, no reaction between Fe(VI) and SMX was observed because no Mössbauer spectra of Fe(III)/Fe(III) as the final product of Fe(VI) reduction were found.

Next, the experiments between Fe(VI) and SMX were extended to pH 11 in phosphate buffer to increase the rate of the reaction. Lowering the pH generally increases the rate of the reactions in the alkaline medium [13, 28, 29]. In this set-up, two solutions were mixed at pH 11 and were frozen in ~ 10 s to 180 s time intervals. Mössbauer spectra of these frozen solutions, shown in Fig. 3, had one singlet and a doublet, which represent Fe(VI) and ferrihydrite, respectively. The identification of ferrihydrite is based on Mössbauer parameters of the doublet. The doublet component increase with the reaction time (see Fig. 3a and b). The final Fe(III) species is consistent with the earlier study on the reaction of Fe(VI) with SMX [20]. The intermediate high-valent iron species were again elusive even at pH 11. It is possible that the intermediate iron species, Fe(V) and Fe(IV), formed during the reaction, were either reacting with SMX or self-decomposing to give Fe(II)/Fe(III) within the time scale (~ 10 s) of the freezing of the mixed sample.

Similarly, the study of Fe(VI) with aniline was carried out in 10 M NaOH and at pH 11. In 10 M NaOH solution, no reaction of Fe(VI) with aniline was observed and Mössbauer spectrum had a single component of Fe(VI). Lowering the reaction solution to pH 11 showed the decay of Fe(VI) with the concomitant growth of the doublet component. Again, no intermediate iron species could be observed. It seems that if Fe(VI)-aniline intermediate formed during the reaction, it must have a life of less than 10 s i.e. time needed to mix the solution, followed by freezing. The doublet component corresponds to Fe(III). This contradicts with the earlier work in which Fe(II) was the final product [22]. It is very likely that Fe(II) produced from the

Fig. 3 Mössbauer spectra of the frozen solutions of the mixture of 0.1 M Fe(VI) and 0.01 M SMX in phosphate buffer at pH 11.0. **a** 10 s; **b** 180 s

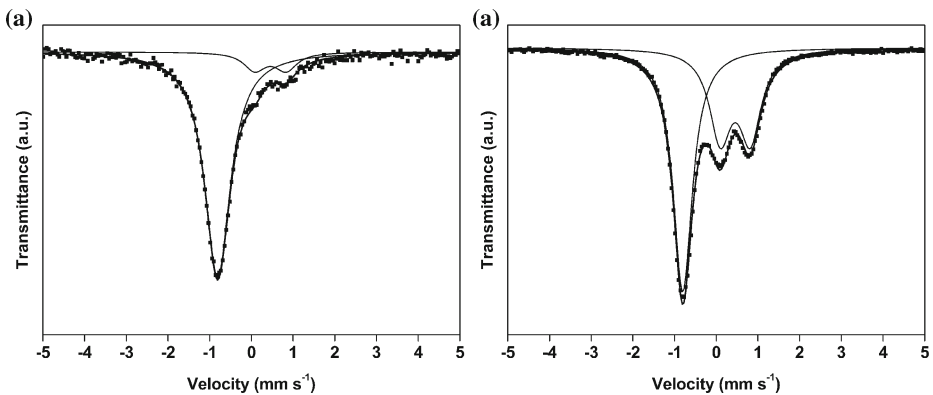
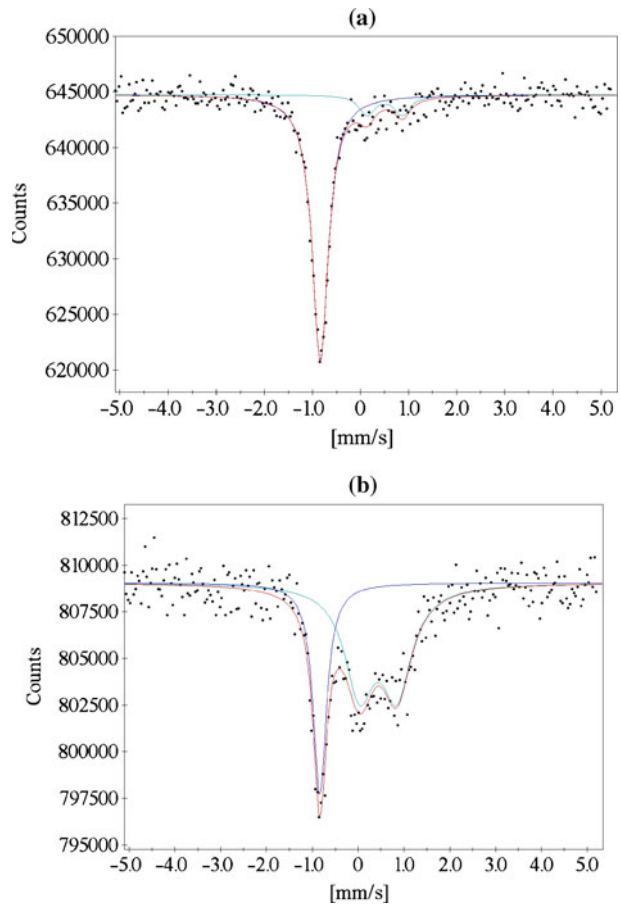


Fig. 4 Mössbauer spectra of the frozen solutions of the mixture of 0.2 M Fe(VI) and 0.2 M aniline in phosphate buffer at pH 9.0. **a** ~ 3 s; **b** 60 s

reaction might have been oxidized by inherent oxygen in the reaction solution. It is known that the oxidation of Fe(II) at such high pH is rapid [30].

Finally, the reaction of Fe(VI) with aniline was studied at pH 9.0, but under anaerobic conditions to make sure no oxygen present in the solution. The reaction was studied at a molar ratio of 1:1 ([Fe(VI)];[aniline]). The Mössbauer spectra, collected after immediate freezing of the solution (~3 s) and 60 s, are presented in Fig. 4. The results were not different from the reaction conducted at pH 11. Besides not observing any of high-valent iron species, expected Fe(II) was also not seen. Because of anaerobic condition, the oxygenation of Fe(II) to form Fe(III) could be ruled out. This suggest the possibility of the reaction between Fe(VI) and Fe(II) under studied conditions, which is fast ($k \geq 10^6 \text{ M}^{-1} \text{ s}^{-1}$) and yielded Fe(III) [31].

It is noteworthy that the Mössbauer parameters of the resultant Fe(III) species are the same in every experiment within experimental error, and are close to that of ferrihydrite. This shows that even at not too high pH (i.e., pH 9.0) the phosphate buffer could not compete with OH⁻ ions in coordinating to iron and the formation of hydroxides/oxyhydroxides were preferred. This process can also stabilize Fe(III) and therefore accelerates decomposition of intermediate oxidation states of iron.

4 Conclusions

Mössbauer spectroscopy approach was shown as an experimental technique to study the mechanism of oxidation of sulfamethoxazole and aniline by Fe(VI). However, freezing of samples of the reaction within three seconds was not sufficient in identifying any of the possible intermediate iron species, Fe(VI)-SMX/Fe(VI)-aniline, Fe(V) and Fe(IV), during the reaction. Further improvement in freezing of reaction samples on the time scale of milliseconds is needed to establish the intermediate iron species, which will allow better understanding of role of high-valent iron, Fe(V) and Fe(IV) species in oxidation reactions of Fe(VI).

Acknowledgements V.K. Sharma acknowledges the partial support of United States National Science Foundation (CBET 1236331) for ferrate research. K. Siskova thanks to the Grant Agency of the Czech Republic for financial support (grant no. P108/11/P657). The authors also gratefully acknowledge the support by the Technology Agency of the Czech Republic “Competence Centres” (project TE01010218), the support by the Innovations—European Regional Development Fund (project CZ.1.05/2.1.00/03.0058 of the Ministry of Education, Youth and Sports of the Czech Republic) and funding from the Operational Program Education for Competitiveness—European Social Fund (projects CZ.1.07/2.3.00/20.0056, CZ.1.07/2.3.00/20.0058 and CZ.1.07/2.3.00/20.0017 of the Ministry of Education, Youth and Sports of the Czech Republic). We thank anonymous reviewers for their comments which improved the paper.

References

1. Yang, B., Ying, G.G., Zhao, J., Liu, S., Zhou, L.J., Chen, F.: *Water Res.* **46**, 2194 (2012)
2. Lee, Y., von Gunten, U.: *Water Res.* **44**, 555 (2010)
3. Hu, L., Martin, H.M., Arce-bulted, O., Sugihara, M.N., Keating, K.A., Strathmann, T.J.: *Environ. Sci. Technol.* **43**, 509 (2009)
4. Hu, L., Page, M., Marinas, B., Shisler, J.L., Strathmann, T.J.: In: *Proceedings—Water Quality Technology Conference and Exposition*, h1/1 (2010)
5. Filip, J., Yngard, R.A., Siskova, K., Marusak, Z., Ettler, V., Sajdl, P., Sharma, V.K., Zboril, R.: *Chem. Eur. J.* **17**, 10097 (2011)

6. Sharma, V.K.: *J. Environ. Sci. Health. Part A, Environ. Sci. Eng. Toxic Hazard. Substance Control* **45**, 645 (2010)
7. Sharma, V.K.: *Environ. Sci. Technol.* **44**, 5148 (2010)
8. Zboril, R., Andrie, M., Oplustil, F., Machala, L., Tucek, J., Filip, J., Marusak, Z., Sharma, V.K.: *J. Hazard. Mater.* **211–212**, 126 (2012)
9. Wood, R.H.: *J. Am. Chem. Soc.* **80**, 2038 (1958)
10. Sharma, V.K.: *Water Sci. Technol.* **55**, 225 (2007)
11. Sharma, V.K., Li, X.Z., Graham, N., Doong, R.A.: *J. Water Supply: Res. Technol., AQUA* **57**, 419 (2008)
12. Sharma, V.K.: *Chemosphere* **73**, 1379 (2008)
13. Anquandah, G., Ray, M.B., Ray, A.K., Al-Abduly, A.J., Sharma, V.K.: *Environ. Technol.* **32**, 261 (2011)
14. Anquandah, G.A.K., Sharma, V.K., Knight, D.A., Batchu, S.R., Gardinali, P.R.: *Environ. Sci. Technol.* **45**, 10575 (2011)
15. Lee, Y., Gunten, U.V.: *Water Res.* **44**, 555 (2010)
16. Lee, Y., Zimmermann, S.G., Kieu, A.T., Gunten, G.V.: *Environ. Sci. Technol.* **43**, 3831 (2009)
17. Anquandah, G.A.K., Sharma, V.K.: *J. Environ. Sci. Health. Part A, Environ. Sci. Eng. Toxic Hazard. Substance Control* **44**, 62 (2009)
18. Sharma, V.K., Sohn, M., Anquandah, G., Nesnas, N.: *Chemosphere* **87**, 644 (2012)
19. Sharma, V.K.: *Coord. Chem. Rev.* **257**, 495 (2013)
20. Sharma, V.K., Mishra, S.K., Nesnas, N.: *Environ. Sci. Technol.* **40**, 7222 (2006)
21. Johnson, M.D., Hornstein, B.J., Wischnewsky, J.: *ACS Symp. Ser.* **985**(Ferrates), 177 (2008)
22. Johnson, M.D., Hornstein, B.J.: *Chem. Commun.* **0**, 965 (1996)
23. Huang, H., Sommerfeld, D., Dunn, B.C., Lloyd, C.R., Eyring, E.M.: *J. Chem. Soc. Dalton Trans.* **0**, 1301 (2001)
24. Sharma, V.K., Siskova, K., Machala, L., Zboril, R.: *AIP Conf. Proc.* **1489**, 139 (2012)
25. Homonnay, Z., Noorhasan, N.N., Sharma, V.K., Szilagyi, P.A., Kuzmann, E.: *ACS Symp. Ser.* **985**, 257 (2008)
26. Perfiliev, Y.D., Sharma, V.K.: *ACS Symp. Ser.* **985**(Ferrates), 112 (2008)
27. Cabelli, D.E., Sharma, V.K.: *ACS Symp. Ser.* **985**(Ferrates), 158 (2008)
28. Sharma, V.K.: *Chemosphere* **73**, 1379 (2008)
29. Sharma, V.K.: *J. Environ. Manag.* **92**, 1051 (2011)
30. Trapp, J.M., Millero, F.J.: *J. Sol. Chem.* **36**, 1479 (2007)
31. Sharma, V.K., Bielski, B.H.J.: *Inorg. Chem.* **30**, 4306 (1991)

Analysis of broadened Mössbauer spectra using simple mathematical functions

Analysis of broadened Mössbauer spectra

A. Cabral-Prieto

Published online: 20 March 2013

© Springer Science+Business Media Dordrecht 2013

Abstract Simulated and experimental broadened Mössbauer spectra are analyzed using several distribution functions. The resolution Hesse and Rübartsch data are reproduced in order to analyze the origin of the oscillations appearing in the recovered distribution function. The lined triangular distribution is used and some of its properties are described. The no implicit n th-nomial distribution function $P(x) = (a\cos(\pi x) + b\sin(\pi x))^n$ is introduced, complementing the Window and Hesse and Rübartsch no implicit distribution functions. This new no implicit distribution function gives similar results of those of Window's method. In addition, the Window method has also been modified by inserting a smoothing factor λ_C . For $0 < \lambda_C < 1$ a hyperfine distribution with low resolution may be obtained; for $\lambda_C > 1$, the opposite is obtained. The Levenberg-Marquardt algorithm is used to solve the involved Fredholm integral equation rather than the typical second order regularized algorithm. From the extracted hyperfine field distribution functions of the Mössbauer spectra of the amorphous and crystallized $\text{Fe}_{70}\text{Cr}_2\text{Si}_5\text{B}_{16}$ magnetic alloy the short range atomic order for the amorphous state of this alloy can be inferred.

Keywords Mössbauer spectroscopy · No implicit and implicit hyperfine distributions · Amorphous alloys · Short range atomic order

1 Introduction

Broad Mössbauer spectra are frequently obtained from materials where slightly different iron sites are present; examples such as amorphous magnetic alloys [1–10];

Proceedings of the Thirteenth Latin American Conference on the Applications of the Mössbauer Effect, (LACAME 2012), Medellín, Colombia, 11–16 November 2012.

A. Cabral-Prieto (✉)

Depto. de Química, Instituto Nacional de Investigaciones Nucleares,

Apdo. Postal 18-1027, Col. Escandón,

Deleg. M. Hidalgo, C. P. 11801, México D. F., México

e-mail: agustin.cabral@inin.gob.mx

nanometric materials with crystal size distribution(s), like goethite [8], hidrotalcites containing iron, stainless steels, etc. [1–10]. The hyperfine parameters of the Mössbauer spectra of these materials (isomer shift δ , quadrupole splitting Δ , and the hyperfine magnetic field H) are usually evaluated as distribution functions ($P(x)$ with $x = \delta$, or Δ , or H) rather than as discrete values. Several methods have appeared in the literature where a sum of magnetic patterns (1) or an implicit distribution like the Gaussian line are used [1, 7, 8, 11]. Others methods assume no implicit expressions for the $P(x)$ distribution. Whereas Window [2] describes $P(x)$ in terms of a Fourier series expansion (FSE), Hesse and Rübartsch [3] use a discrete step function. According to this line of thought, the n th nomial distribution function $P(x) = (a\cos(\pi x) + b\sin(\pi x))^n$ assumes neither a previous knowledge of the $P(x)$ distribution, and is introduced in this study. The resulting distributions from this new function are practically similar to those obtained from the Window method [3]. The implicit lined triangle distribution function is also introduced in this study. In addition to these new proposed no-implicit and implicit distribution functions the Window method has been modified by inserting a smoothing factor λ_C which can take the values $0 > \lambda_C \geq 1$. For a highly resolved distribution function a $\lambda_C > 1$ is required. This smoothing factor multiplies the trigonometric argument of the Cosine or Sine function appearing in the Window method [2].

Generally speaking, one can get practically the same results using anyone of these three no-implicit distributions functions (Window, Hesse and Rübartsch, and present methods). Particularly, the Hesse and Rübartsch method is faster than the others but it is basically limited to one parameter, the number of points of the distribution (NSUB), to get a well resolved distribution. The Window method originally had the number of terms of the FSE in order to obtain a well resolved distribution. The introduction of the smoothing factor λ_C in the present work gives an additional parameter in order to optimize a solution. Similarly the new n th-nomial distribution function depends on the number of terms $(n + 1)$ of the distribution. In addition to this, the later no implicit distribution handles even and odd functions simultaneously. This property would allow studying them in a future work in order to see if it is possible to reduce the oscillations that appear in any solution of these no implicit methods.

2 Experimental

The resolution Hesse and Rübartsch data consisting of a magnetic sextet modified by two Gaussian distribution functions centered at 17.5 and 20 T of standard deviation $\sigma = 0.85$ T each are reproduced [3]. The above simulated spectrum and those of the amorphous and crystallized soft magnetic $\text{Fe}_{77}\text{Cr}_2\text{Si}_5\text{B}_{16}$ alloy (S3A alloy from Metglas) are analyzed by using the unmodified and modified Window methods [2] and the new proposed distribution function.

3 Methodology

Present analysis assumes the thin absorber approximation where the resonance line is a Lorentzian distribution of FWHM $\Gamma = 0.194$ mm/s. In the transmission

Mössbauer set up, a broadened magnetic Mössbauer spectrum can be represented by the Fredholm integral of the first kind as

$$S_{calc} = \int_c^d P(B) L_6(v, B) dB, \tag{1}$$

where $S_{calc}(v)$ is the calculated spectrum as a function of the relative velocity between the absorber and Mössbauer source. $L_6(v, B)$ stands for the magnetic sextet of normalized Lorentzian lines and $P(B)$ is the unknown probability distribution function of the hyperfine magnetic field B . The condition $\int_c^d P(B)dB = 1$ has to be met if quantitative information is required from the measured spectrum $S_m(v)$.

The solution of integral equation (1) needs a careful numerical treatment because the resulting hyperfine distribution(s) and the fitted spectrum may posses an oscillatory behavior due to statistical fluctuations on the experimental data set $S_m(v)$ or rounding errors (3, 7, 9). In order to solve this problem several regularized algorithms are at hand. Singular Value Decomposition (SVD), Truncated Singular Value Decomposition (TSVD), Generalized SVD (GSVD), the Tikhonov-Arsenine regularization or the Philips-Twomey regularization methods are some of them. The Tikhonov regularization methods are classified as zero, first and second order regularization algorithms. Any of these algorithms regularizes the ill-posed problem derived from the solution of integral equation (1). From the author’s perspective, the preferred algorithm used in Mössbauer spectroscopy is the Philips-Twomey or Tikhonov second order regularization method after proposing it by Hesse and Rübartsch [3]. The zero and first order regularization algorithms, or the SVD, TSVD GSVD have been little explored. The Levenberg-Marquadt (LM) algorithm, which is the standard routine to solve non-linear problems, may also be considered as the Tikhonov zero order regularization method, and is used in the present work. The resulting normal equations of this algorithm may be written as

$$(J^T J + \lambda_{LM} I) \Delta x = J^T b, \tag{2}$$

where J represents the Jacobian matrix and J^T its transpose, λ_{LM} is the Levenberg-Marquardt factor that controls the searching route to obtain the “best solution” between the Gauss-Newton and the Steepest-Descent methods, I is the identity matrix; λ_{LM} is an internal parameter of the computing program and one has not to worry about it; b represents the weighted residuals between the measured data $S_m(v)$ and the calculated $S_{calc}(v)$ ones. Expression (2) is practically the same as that of the standard form of Tikhonov zero order regularization algorithm

$$(J^T J + \lambda_T I) \Delta x_T = J^T b \tag{3}$$

The goal of the Tikhonov λ_T factor in (2) is to provide a “smooth solution” of the desired hyperfine $P(x)$ distribution and of the fitted spectrum $S_c(v)$. In this case, the Tikhonov λ_T factor is user defined. Technically, the effect of both the LM and Tikhonov factors, λ_{LM}, λ_T in (2) and (3), respectively, is to dampen the contributions of small singular values in the solution of the $J^T J$ matrix.

Thus the Levenberg-Marquadt algorithm can, under certain conditions, be considered the same to the Tikhonov zero order regularization. Thus, a first introspection of the solutions that can provide the LM algorithm is presented using several distribution functions.

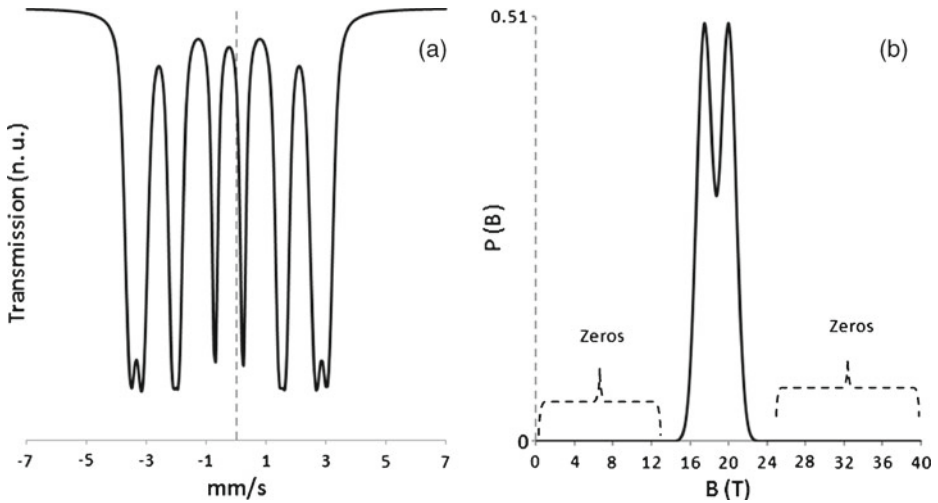


Fig. 1 Hesse and Rübartsch's data [3]. (a) A distributed sextet by (b) two Gaussian lines, centered at 17.5 and 20 T

4 Results

4.1 Hesse and Rübartsch's data

The resolution test data of Hesse and Rübartsch's paper is reanalyzed. Figure 1 shows the corresponding data of example 3. (ii) from reference [3], where a magnetic sextet is distributed by a two Gaussian shaped functions ($P(B)$), centered at the magnetic field values $B = 17.5$ and 20 T and having a standard deviation $\sigma_H = 0.85$ T each, as shown in Fig. 1a and b. A first observation must be made from the two Gaussian distribution function, Fig. 1b: the plotted distribution function $P(B)$ has two regions of zeros as indicated by the keyets.

These zeros appear from 0.0 to 12.5 T and from 25 to 40 T. That is, the integration limits of integral equation (1) should be $c = 12.51$ and $d = 25.1$ T only.

The recovered distribution function $P(B)$ from Fig. 1a when applying the unmodified Window method [3] as suggested in reference [3], using the limits $c = 0$ and $d = 40$ in the integral equation (1), and using 15, 25 and 35 terms of the FSE, is shown in Fig. 2. The resulting distributions have oscillations as those shown in reference (3). The best fit is obtained when using 35 terms of the FSE but still small oscillations are present in the resulting distribution, Fig. 2c'. A little higher oscillations appear if the Lorentzian width of the sextet is fixed to its actual value ($W_L = 0.1926$ mm/s [3]). Such oscillations are removed if the c and d integral limits are, for example 12.5 and 25 T, respectively, or if they are calculated by the program as shown in Fig. 3a', respectively. Two presentations of the resulting distribution can be made, the typical superimposed distribution (Fig. 3a' and the separated one, Fig. 3b'). The squared chi fitting criterion is improved by two orders of magnitude if the integral limits are guessed and the distributions are separated, Fig. 3b'. In the last two cases the line width of the sextet was also evaluated and was recalculated with zero error as shown in the Fig. 3b' case.

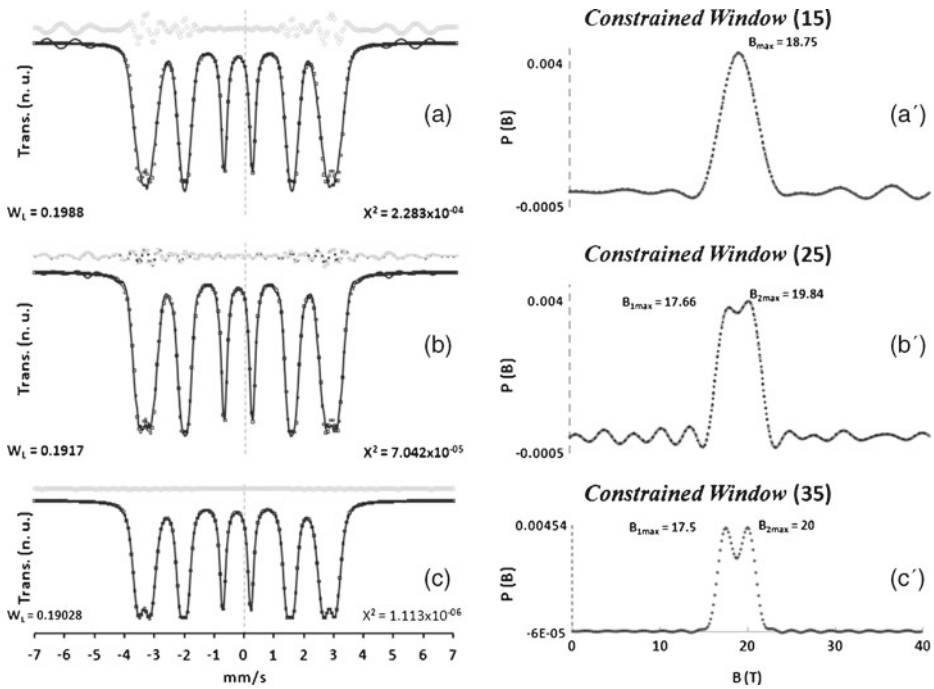


Fig. 2 Hyperfine field distributions by Hesse and Rübartsch [3] using the Window method [2]. On the top of each left figure the un-normalized residuals are plotted. The Lorentzian width W_L was evaluated and was not recovered

The case for which the Gaussian distribution function is replaced by a triangular distribution function is shown in Fig. 3c'. Firstly, note that in this case a single parameter (the number shown in parenthesis in these figures) is only required to define a triangular distribution function. In the present case, the computing program also requires a single parameter to produce both triangles as shown in Fig. 3c'. Thus this triangular distribution speeds up any calculation as compared to those using the Window or other methods. Secondly, it can be noticed from the small residuals that this triangular distribution function is not a bad approximation to the original Gaussian distribution $P(B)$. The integration limits are also evaluated by the program and in this case the possibilities of oscillations in the fitted spectrum and distribution are also removed.

4.2 S3A magnetic alloy

Following the above strategy, i. e. optimizing the integral limits to prevent any spurious oscillations, the CXMS and transmission spectra of the amorphous soft magnetic alloy S3A, treated at 50C/20' and 430C/20', respectively, are next analyzed. Figure 4 shows two typical hyperfine field distributions (HFD) from the amorphous state of the alloy when using the unmodified [2] and modified Window methods with 6 terms of the FSE (and $\lambda_c = 1.0$) and 12 terms of the FSE (and $\lambda_c = 1.1109$), either evaluating or fixing the intensity ratios of lines two and five (I25) of the magnetic sextet.

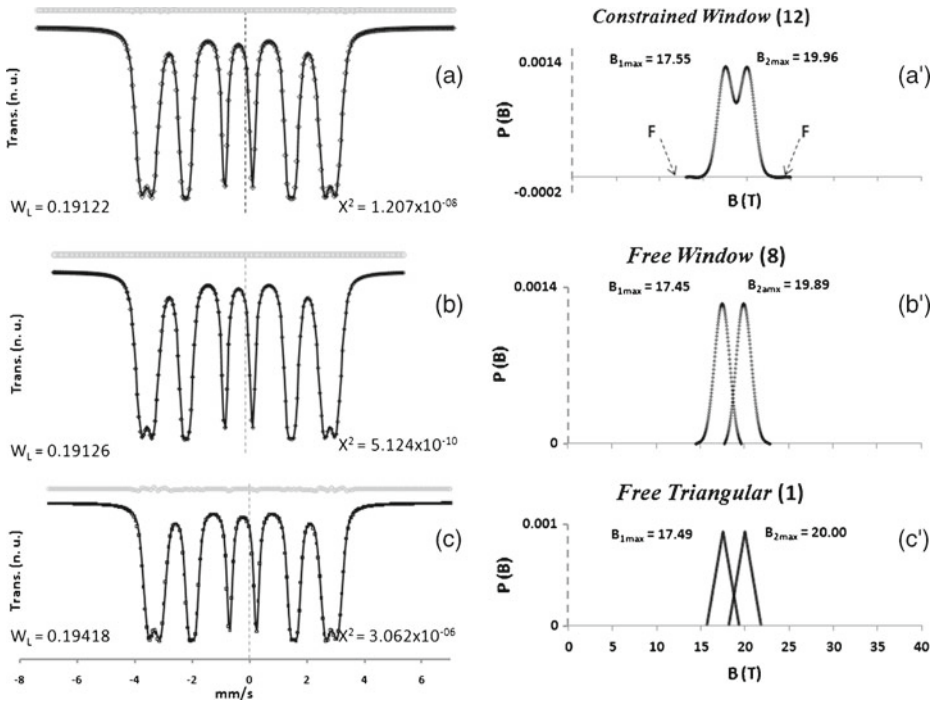


Fig. 3 Oscillations free hyperfine distributions obtained by (a) fixing the c and d integral limits, using 12 terms of the FSE, or (b) guessed using 8 terms of the FS only. The distribution can be obtained as (a) superimposed or (b and c) separated one

A single Gaussian distribution is suggested from Fig. 4a'. A more complex distribution is obtained if 12 terms of the FSE and λ_c is evaluated. The latter distribution will be named as the low resolved hyperfine field distribution (LR-HFD). Whereas Fig. 4a' may suggest a single phase, i. e., the amorphous phase of the alloy, Fig. 4b' might suggest a set of Fe-Cr-Si-B crystalline phases.

From the Mössbauer spectroscopy, and particularly from the LR-HFD, still remains ambiguous if the experimental Mössbauer spectrum of metallic glasses, like the S3A alloy, indeed originates from the amorphous phase (Fig. 4a') or not (Fig. 4b').

A similar LR-HFD was reported by Le Caer and Dubois in 1979 arising from the amorphous alloy $Fe_{79.5}Si_{1.5}B_{19}$ [7]. As a result of this, a great deal of research has been carried out to elucidate the local atomic structure around the iron, boron and phosphorus atoms of these metallic glasses in order to be able to interpret the spectral features of Fig. 4b' suggesting the presence of crystalline material [7–14]. Nowadays is generally believed that the local structure around the boron atoms in metallic glasses possess short-range atomic-order (SRAO) rather than short-range atomic-disorder (SRAD). Research work in this area is still in progress to define such a matter (13, 14). The SRAO perception came after studying ^{10}B NMR spectroscopy in some metallic glasses containing ^{10}B , where sharp NMR peaks arise from different supposedly amorphous Fe-B phases [8, 13].

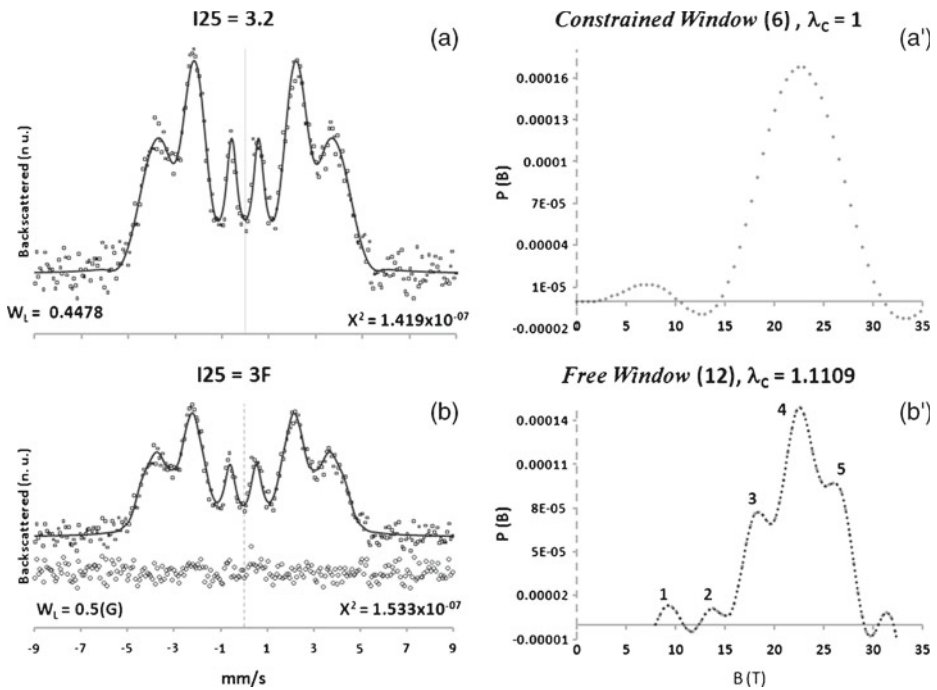


Fig. 4 (a) Fitted CXMS spectrum of the amorphous alloy using the unmodified Window’s method ($\lambda_c = 1$), (a’) an unresolved hyperfine field distribution is obtained when using six terms of the FSE. (b) Fitted CXMS spectrum of the amorphous alloy using the modified Window’s method ($\lambda_c = 1.1109$), (b’) a low resolved hyperfine field distribution is obtained when using 12 terms of the FSE

The question that arose at Le Caer and Dubois’s time (1979) was: Are real the spectral features of the LR-HFD as shown in Fig. 4b’? or they are the product of mathematical artifacts? As far as the author understands, these spectral features appearing in Fig. 4b’ have not been answered quite satisfactorily.

In the present case, the mathematical artifacts (spurious oscillations) can mostly be discharged from Fig. 4b’ due to the fact that the integral limits are optimized and minimal oscillations would be expected. The statistical nature of the present experimental data may also produce additional oscillations. However, this also can be ruled out because the statistical quality of the Mössbauer data of Le Caer and Dubois’s paper [7] is better than in the present case, and in spite of this the obtained distributions and the fitted spectrum are practically the same as those reported by Le Caer and Dubois [7]. In addition to this, no matter if a zero order or a second order regularized algorithm is used. Thus, in order to give, from the Mössbauer point of view, support to the LR-HFD structure of Fig. 4b’, the transmission Mössbauer spectrum (TMS) of the heat treated S3A alloy at 530C/20’ was obtained, which is shown in Fig. 5b.

This TMS was fitted using the trigonometric n th-nomial distribution function $P(x) = (a\text{Cos}(\pi x) + b\text{Sin}(\pi x))^n$ with $n = 29$. The resulting coefficients of this trigonometric distribution function are evaluated as simple parameters by the program. Take the example case for $n = 2$ where the resulting coefficients are: $a^2, 2ab,$

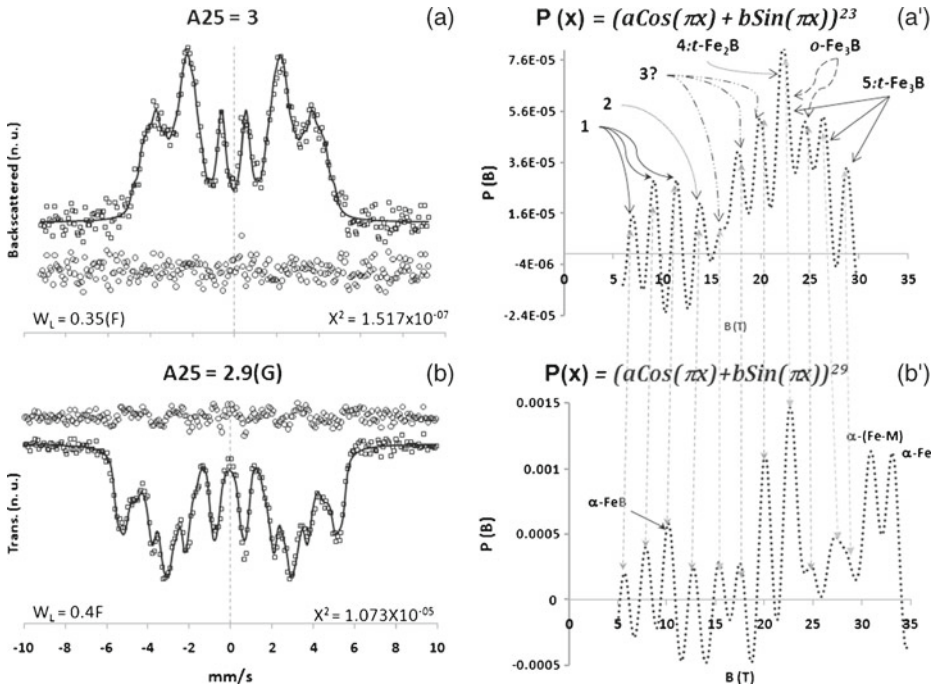


Fig. 5 (a) CXMS Mössbauer spectrum of the amorphous alloy fitted using the trigonometric sum with an exponent $n = 23$; (b) Transmission Mössbauer spectrum of the crystallized alloy fitted using the n th-binomial expansion distribution with $n = 29$

b^2 and the corresponding numerical values are: 1, 2, 1, respectively, with $a = 1$ and $b = 1$. The evaluated coefficients generally differ from the preceding whole numbers.

For comparison purposes, the fitted Mössbauer spectrum and the resulting HFD of the amorphous alloys are also presented in Fig. 5a and a'; in this case a 23th-nomial trigonometric function was used and a high resolved HFD (HR-HFD) is now shown for both these cases, Fig. 5a' and b' having practically the same peak structure for fields lower than 30 T. A small shift is observed between these peaks only. Is it a coincidence such a peak matching? Or is it an evidence of the short-range atomic structure of the amorphous state of the alloy?

Large oscillations with negative values appearing in Figs. 4 and 5b's should not be considered, they were enhanced in order to obtain HR distributions containing the typical information of these alloys [14, 15]. Negative values can be eliminated but LR distributions are obtained which are not useful for the present discussion.

Thus the LR-HFD in Fig. 4b' may be rationalized as follows:

- (i) The small broad peak at 9.25 T, peak 1 shown in the LR-HFD of Fig. 4b', and a first group of three peaks, gathered by curved arrows as shown in the HR-HFD of Fig. 5b', located at 5.47, 7.81 and 10.16 from which an average peak value of 7.81 T is obtained. This average value deviates -15.53% the peak 1 position in Fig. 4b'. If this average value is taken from the HR-HFD of the amorphous material such deviation is less than 1%. Broken lines between peaks of Figs. 4 and 5b' show the corresponding shifts.